AJNR

Dynamic Contrast-enhanced T2*-weighted MR Imaging of Recurrent Malignant Gliomas Treated with Thalidomide and Carboplatin

Soonmee Cha, Edmond A. Knopp, Glyn Johnson, Andrew Litt, Jon Glass, Michael L. Gruber, Stanley Lu and David Zagzag

AJNR Am J Neuroradiol 2000, 21 (5) 881-890
http://www.ajnr.org/content/21/5/881

AJNR Am J Neuroradiol 21:881–890, May 2000

Dynamic Contrast-enhanced T2*-weighted MR Imaging of Recurrent Malignant Gliomas Treated with Thalidomide and Carboplatin

Soonmee Cha, Edmond A. Knopp, Glyn Johnson, Andrew Litt, Jon Glass, Michael L. Gruber, Stanley Lu, and David Zagzag

BACKGROUND AND PURPOSE: **Dynamic, contrast-enhanced MR imaging has allowed quantitative assessment of cerebral blood volume (CBV) in brain tumors. The purpose of our study was to compare postcontrast T1-weighted imaging with dynamic, contrast-enhanced T2*-weighted echo-planar imaging in the evaluation of the response of recurrent malignant gliomas to thalidomide and carboplatin.**

***METHODS*: Serial MR imaging was performed in 18 consecutive patients with recurrent malignant gliomas receiving both thalidomide and carboplatin for 12-month periods. Six patients undergoing carboplatin therapy alone were chosen as control subjects. Conventional postcontrast T1-weighted images were compared with relative CBV (rCBV) maps calculated on a pixel-by-pixel basis from dynamic echo-planar imaging data. Tumor progression was evaluated clinically using established criteria for malignant gliomas. Studies were performed at 2- to 3-month intervals, and imaging and clinical findings were compared.**

***RESULTS*: Tumor response to treatment, based on clinical findings, did not correlate well with conventional imaging findings. The rCBV values decreased significantly in all patients between the start of therapy and the first follow-up in the study group, but not in the control group. The difference in rCBV values between the clinically stable and the progressive group at 12-month follow-up was statistically significant, with the progressive group having higher values.**

***CONCLUSION*: Dynamic, contrast-enhanced MR imaging is a valuable adjunct to conventional imaging in assessing tumor activity during antiangiogenic therapy, and correlates better than conventional studies with clinical status and response to therapy.**

Conventional chemotherapy, targeting mitotic activity, is rarely effective in treating recurrent gliomas (1–4). Angiogenesis is one of the most malignant features of recurrent high-grade glioma, and the recent emergence of antiangiogenic agents offers the hope of more effective treatment. Thalidomide has recently been approved for limited use in dermatologic complications of leprosy. Thalidomide's antiangiogenic properties have been well documented (5–7) and it has shown activity against gliomas in phase I trials (8, 9).

With advances in adjuvant chemotherapy, patients with malignant gliomas are living longer and there is a need for more sophisticated imaging surveillance of tumor progression. Clearly, a method for monitoring the efficacy of antiangiogenic agents would aid both research and treatment planning. It is often difficult to evaluate progression of malignant gliomas on conventional postcontrast T1-weighted MR images alone; however, because abnormal enhancement is nonspecific and cannot differentiate tumor progression from therapy-related changes. Dynamic, contrast-enhanced T2*-weighted echo-planar MR imaging has previously been shown to be helpful in assessing tumor vascularity (10–12) and may fill this need. The purpose of our study was therefore to compare postcontrast T1-weighted imaging with dynamic, contrast-enhanced T2*-weighted echo-planar imaging in monitoring the response of recurrent malignant gliomas to treatment with thalidomide and carboplatin.

Received June 14, 1999; accepted after revision December 6.

From the Departments of Radiology (S.C., E.A.K., G.J., A.L., S.L.), Neurosurgery (E.A.K.), Neuro-oncology (J.G., M.L.G.), and Pathology, Division of Neuropathology (D.Z.); and the Kaplan Cancer Center (E.A.K., M.L.G., D.Z.), New York University Medical Center, New York.

Presented at the annual meeting of the American Society of Neuroradiology, Philadelphia, May 1998.

Address reprint requests to Soonmee Cha, MD, Department of Radiology, NYU Medical Center, MRI Division, 530 First Ave, New York, NY 10016.

Methods

MR imaging studies were performed in 18 consecutive patients with recurrent malignant gliomas who were enrolled in a trial to investigate treatment with thalidomide and carboplatin (9). All 18 patients received external beam radiation at the time of their initial diagnosis after surgical resection of the original tumor. The institutional board of research associates at our institution approved the treatment protocol. The following criteria were used for patient selection: 1) the presence of recurrent high-grade gliomas confirmed by biopsy or tumor resection at the time of suspected clinical recurrence; 2) patient's age greater than 18 years; 3) patient's Karnofsky performance status greater than 70%; 4) previous chemotherapy limited to nonplatinum agents; 5) no prior treatment with thalidomide; and 6) patient's life expectancy at least 15 weeks. The patient group consisted of nine women and nine men, 33 to 77 years old (mean age, 50 years). None of the patients had received prior adjuvant chemotherapy with thalidomide or carboplatin. Informed consent was obtained from all patients.

Six patients (three men and three women, 27–64 years old, mean age, 46 years) undergoing high-dose carboplatin therapy without thalidomide for recurrent malignant gliomas served as a control group. Like the study group, the control subjects had all received irradiation and nonplatinum chemotherapy at the time of initial diagnosis of malignant glioma.

MR imaging was performed at the start of therapy to determine initial tumor size and location, contrast enhancement patterns, and perfusion imaging findings. During therapy, follow-up imaging was performed every 2 to 3 months depending on the clinical status of the patient. The following MR imaging protocol was used: localizing sagittal T1-weighted images were followed by T2-weighted (3400/119/1 [TR/TE/excitations]) and fluid-attenuated inversion recovery (6500/105/1; inversion time, 2500) images of the brain. From the T2-weighted images, tumor location and size were estimated, and the slice positions of the inferior and superior margins of the tumor were recorded. Perfusion-weighted dynamic, contrast-enhanced images were then acquired as described below, and, finally, postcontrast axial T1-weighted images were obtained.

Perfusion data were obtained by acquiring a series of echo-planar images immediately before, during, and after injection of a bolus of gadopentetate dimeglumine. The echo-planar imaging technique consisted of a T2*-weighted (1000/54/1) sequence with a flip angle of 90° and a lipid-suppressed blipped sequence (ie, the phase-encoding gradient was applied in short pulses rather than continuously). Based on tumor size and position estimated from the T2-weighted images, five to seven slices, 5- to 7-mm thick (gap, 0–2 mm) were selected to cover the entire tumor volume. The first 10 echo-planar imaging sequences were obtained before the contrast injection to establish a precontrast baseline. At the 10th acquisition, contrast material (0.1 mmol/kg) was injected by power injector at a rate of 3 or 5 mL/s (total volume of 20 mL) through an 18- or 20-gauge angiocatheter, followed immediately by 20 mL of continuous saline flush.

The raw echo-planar images were transferred to a Sun SPARC 5 station (Sun Computer, Mountain View, CA) for processing. All software programs for postprocessing were developed in house by using C and IDL programming language (Research Systems, Inc, Boulder, CO) (13). Details of data processing are fully described by Knopp et al (10), and only a summary will be given in this article. During the first pass of the paramagnetic contrast bolus, there is a drop in signal intensity on T2*-weighted images. Gadolinium concentration can be inferred from signal intensity changes to obtain a plot of tissue gadolinium concentration over time. The area under this curve is proportional to the regional cerebral blood volume (CBV) (14). Correction for contrast recirculation and leakage (which invalidate the CBV calculation) was performed by subtracting a baseline from under the contrast bolus. The beginning and end of the bolus were defined as the images at which the signal came within 1 SD of the mean pre- and postbolus signal, respectively. The baseline drawn between these two points was then subtracted from the signal.

Diagnosis and outcome in the 18 patients with recurrent malignant glioma who received both thalidomide and carboplatin

Case No.	Age (y)/Sex	Pathologic Diagnosis	Clinical Outcome at 12 Months
1	50/F	GBM	D
2	42/F	GBM	D
3	36/M	GBM	D
4	77/F	GBM	D
5	62/M	GBM	D
6	46/M	AOA	R
7	48/F	GBM	R
8	37/M	GBM	R
9	64/F	GBM	R
10	55/M	GBM	R
11	61/F	GBM	S
12	58/M	GBM	S
13	34/F	GBM	S
14	33/F	GBM	S
15	37/M	AGG	S
16	50/F	AA	S
17	50/M	GBM	S
18	59/M	GBM	S

Note.—GBM indicates glioblastoma multiforme; AOA, anaplastic oligoastrocytoma; AGG, anaplastic ganglioglioma; AA, anaplastic astrocytoma; D, deceased; R, relapsed; S, stable.

The constant of proportionality is unknown in these calculations, so that CBV must be expressed relative to an internal reference, such as the normal contralateral white matter. We refer to these values as relative CBV, or rCBV. Additionally, a color overlay map was formed that showed the maximum signal intensity drop during the passage of contrast bolus. The color overlay was used both for a qualitative assessment of perfusion changes and as a roadmap to select regions of interest (ROIs) for rCBV measurements. At least 10 rCBV measurements were obtained in different ROIs within the lesion to yield a mean rCBV value. Mean rather than maximum rCBV values were chosen to better reflect the overall degree of vascularity. Serial rCBV measurements were recorded during the 12-month follow-up. Paired *t*-tests were used to determine whether differences in measured rCBV values were significant.

Two neuroradiologists evaluated serial conventional MR images for tumor size, the extent and pattern of contrast enhancement, and the extent of peritumoral T2 signal abnormality. An estimate of tumor size was obtained by taking the product of the two largest perpendicular tumor diameters. Tumors that showed a 25% increase or decrease in size between sequential scans were characterized as progressively enlarging or regressing, respectively, regardless of changes in contrast enhancement pattern.

Clinical evaluation of each patient was performed by two neurooncologists. All patients were monitored for toxicity while undergoing treatment, and assessment of overall neurologic status was recorded at each follow-up visit. Karnofsky performance status was assessed at each follow-up, and clinical symptoms and signs of tumor progression were closely monitored. Clinical response was based on criteria proposed by Macdonald et al (15) and was divided into four categories: 1) complete response, total disappearance of all enhancing or nonenhancing tumor or edema on MR images for at least 4 weeks; 2) partial response, a greater than 50% diminution in tumor size on MR images, with improvement or stability of neurologic status, lasting for 4 weeks or more; 3) stable dis-

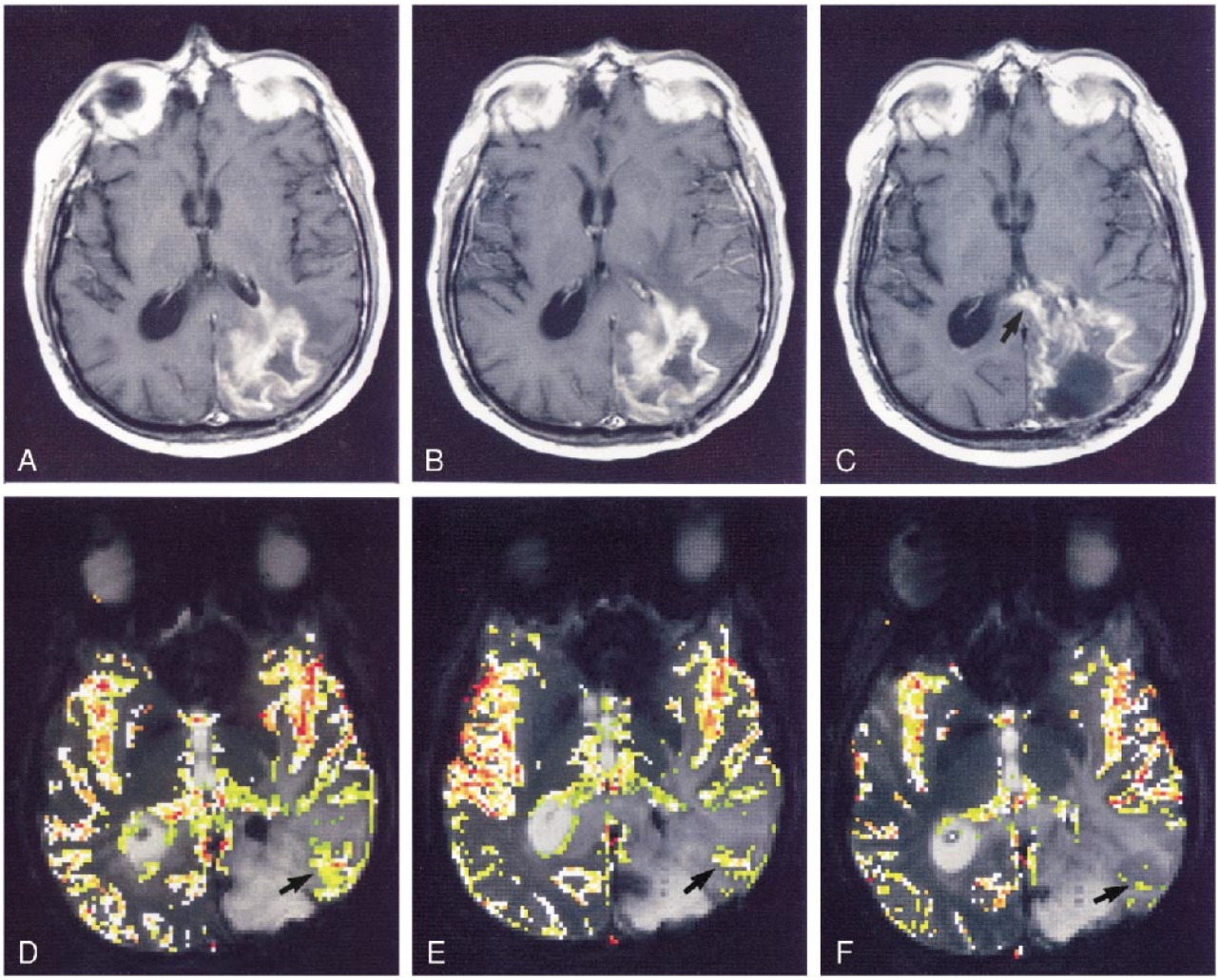

FIG 1. Case 12: 58-year-old man with GBM treated with carboplatin and thalidomide, without concomitant steroid therapy.

A–C, Postcontrast T1-weighted images. At the start of therapy, an irregularly enhancing mass is seen in the left parietooccipital region (*A*). At 4-month follow-up, there is mild interval increase in contrast enhancement (*B*). At 8-month follow-up, a new area of abnormal contrast enhancement is seen in the splenium of the corpus callosum (*arrow*) as well as lateral periatrial and ventricular involvement (*C*).

D–F, Corresponding color overlay images. At the start of therapy, a focal area of hyperperfusion (*arrow*) is seen in the lateral aspect of the left parietooccipital tumor (*D*). At 4-month follow-up, there is interval decrease in the perfusion abnormality in the same region (*arrow*) (*E*). At 8-month follow-up, almost complete resolution of the perfusion abnormality is noted in the left parietooccipital lobe (*arrow*). There is no abnormal perfusion corresponding to the contrast enhancement within the splenium of the corpus callosum. Although conventional imaging findings are consistent with tumor progression, a lack of perfusion abnormality suggests otherwise. The patient was clinically stable at 12- and 16-month follow-up examinations (*F*).

ease, a 0% to 50% reduction in tumor size, with improvement or stability of neurologic status, lasting 4 weeks or more; and 4) progressive disease, an increase in tumor size on MR images or clinical worsening despite lack of progression on MR studies. All responses were defined in a setting of stability or improvement in the neurologic examination with stable or decreased steroid requirement.

Results

None of the patients reported any adverse reaction to rapid power injection of the contrast material. Susceptibility artifacts inherent in echo-planar imaging did not interfere with imaging or postprocessing.

The pathologic diagnoses among the 18 patients were as follows: glioblastoma multiforme (GBM) (n = 15), anaplastic astrocytoma (n = 1), anaplastic oligoastrocytoma (n = 1), and anaplastic ganglioglioma (n = 1). Among the control group of six patients who received only carboplatin, four had GBM, one had anaplastic oligoastrocytoma, and one had anaplastic astrocytoma. At the time of clinical recurrence, 15 patients underwent partial debulking resections and three had biopsies. In the control group, two patients had partial debulking resections and four had biopsies.

The clinical outcome in the 18 patients in the study group at 12-month follow-up was as follows:

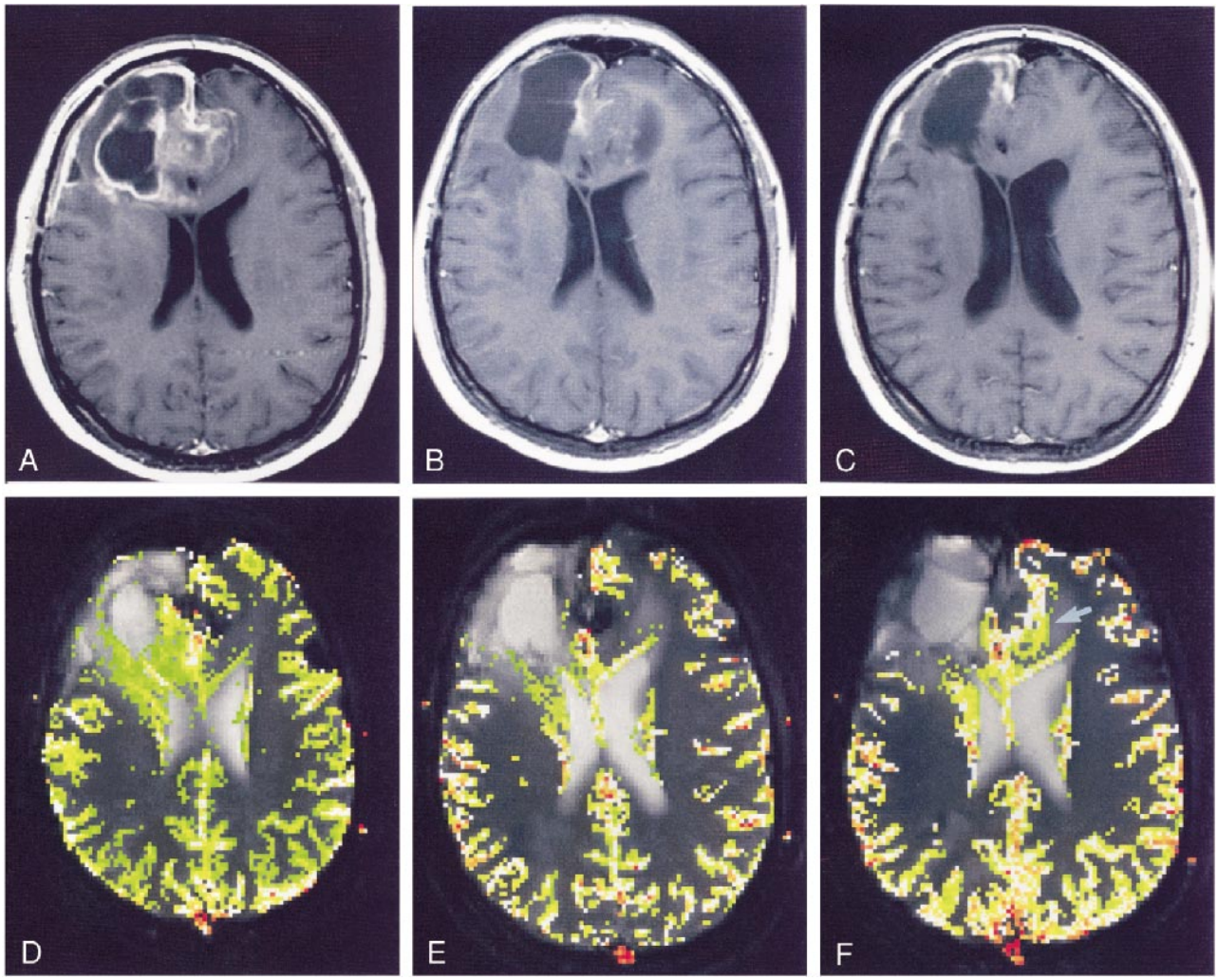

FIG 2. Case 3: 36-year-old man with bifrontal GBM treated with carboplatin and thalidomide, without concomitant steroid therapy.

A–C, Postcontrast T1-weighted images. At the start of therapy, a heterogeneous, irregularly enhancing right frontal GBM with areas of necrosis extends into the contralateral frontal lobe (*A*). At 3-month follow-up, there is a decrease in contrast enhancement within the bifrontal tumor (*B*). At 7-month follow-up, there is further decrease in contrast enhancement (*C*).

D–F, Corresponding color overlay images. At the start of therapy, a focal area of hyperperfusion is seen in the medial aspect of the right frontal tumor (*D*). At 3-month follow-up, there is an interval decrease in the perfusion abnormality in the right medial frontal lobe tumor (*E*). At 7-month follow-up, a new focus of hyperperfusion is seen in the left medial frontal lobe (*arrow*) without corresponding abnormality on conventional T1-weighted image (*F*).

five had died, five had progression of symptoms, and eight remained stable (see Table on page 882). Four of five patients who relapsed clinically underwent reoperation at our institution. In the control group, four died and two remained clinically stable.

During the 12-month follow-up period, all but one patient showed a progressive increase in the extent of conventional contrast enhancement within the tumor. In most tumors, there was a distinctive pattern of change in contrast enhancement during therapy. The enhancement filled in centripetally, from the periphery to the center, replacing the central portion of the necrotic and/or postsurgical cavity with solid contrast-enhancing tissues. Figure 1A–C shows a typical enhancement pattern in a patient with progressive increase in enhancement over three follow-up examinations. Despite these findings, suggestive of tumor progression, the patient remained clinically stable (ie, there were no signs or symptoms of increasing intracranial mass effect or progression of focal neurologic deficit, and no further deterioration). Clinical status did correlate with the perfusion findings (Fig 1D–F), however, which showed no increase in perfusion abnormality at follow-up with stable rCBV values. None of the eight patients in the stable group showed statistically significant increases in rCBV during the therapy period, despite progressive increases in conventional contrast enhancement.

In one patient, there was a significant decrease in the contrast-enhancing portion of the right frontal tumor during therapy, suggestive of tumor regression (Fig 2A–C). MR perfusion imaging, however, disclosed new areas of hyperperfusion in the contralateral frontal lobe, contradicting the conven-

tional imaging findings (Fig 2D–F). This patient had rapid clinical deterioration, leading to death soon after the third follow-up examination. Another patient in the relapsed group had only mild progression of abnormal enhancement in the left medial frontal lobe (Fig 3A–C). There was, however, a marked increase in perfusion abnormalities (Fig 3D–F) over a 9-month period, correlating well with the patient's deteriorating clinical status.

Overall tumor size, as estimated by the tumor's largest cross-sectional area, progressively increased in five (28%) of the 18 patients, decreased in one, and did not significantly change in the remaining 12. None of the patients had greater than a 50% reduction in tumor size over the course of 12 months. Those five patients with increasing tumor size also had progressive increase in peritumoral hyperintense signal abnormality on T2-weighted images and two of the patients had new sites of abnormal contrast enhancement remote from the original tumor.

Study Group versus Control Group

Calculated rCBV values at each follow-up examination for the thalidomide and carboplatin group and for the control group (carboplatin only) are plotted in Figures 4 and 5, respectively. In the control group, the initial and first follow up rCBV values were 7.17 ± 1.88 (mean ± SD; range, 4.73–9.27) and 6.33 ± 2.26 (range, 2.63–9.53), respectively. This difference in rCBV was not statistically significant ($P = .150$). In the study group, on the other hand, the mean rCBV was 6.55 ± 2.55 (range, 2.92–13.0) at the start of the therapy and had fallen to 3.40 ± 1.89 (range, 1.26–8.06) at the first follow-up examination at 2 months. This difference was statistically significant ($P = .0014$). In the control group, rCBV values progressively increased throughout the study.

Clinically Stable versus Relapsed Group Receiving Thalidomide and Carboplatin

The difference in mean rCBV between the initial and the first follow-up was statistically significant ($P = .0014$) among the clinically stable and the relapsed groups (Fig 6). At 12 months (ie, the fifth examination), the mean rCBV of the clinically stable and relapsed groups was 2.19 ± 0.65 (range, 1.22–3.51) and 6.56 ± 1.36 (range, 5.11–8.22), respectively. The difference in rCBV was statistically significant ($P = .0161$). Over the course of 12 months, the patients in the clinically progressive group showed sequential increases in rCBV measurements relative to the first posttreatment value. By contrast, the clinically stable group showed minimal increases in rCBV during this period.

Deceased Group

In the five patients who died, the initial and final rCBV values were 7.97 ± 0.95 (range, 7.02–9.42) and 3.72 ± 1.56 (range, 2.21–5.69), respectively. One patient died of myocardial infarction, and the other four died of presumed progression of brain tumor. None of the patients underwent postmortem examination.

Pathologic Findings

Pathologic analysis of four of the five patients in the progressive group who had surgery showed further progression of malignant glioma, as evidenced by marked cellular pleomorphism, a high mitotic index, necrosis, and vascular hyperplasia. In addition, the neocapillaries demonstrated bizarre morphology and chronic inflammatory changes around the vascular endothelium in a pattern consistent with radiation-induced fibrinoid necrosis. There was marked hyalinization and extracellular matrix deposition surrounding the vascular endothelium, pathologic features that are not typical of recurrent high-grade gliomas. Figure 7 illustrates an azocarmine stain from a patient (case 7) with a recurrent GBM who was treated with carboplatin and thalidomide that shows multilayered reduplication of the basal lamina around a microvessel.

Discussion

Without exception, all high-grade gliomas recur at some point, despite aggressive therapy (4, 16). Two distinct but probably interrelated pathologic events accompany recurrence of high-grade glial neoplasms: angiogenesis and infiltration (4, 16, 17). Although it is not clear whether angiogenesis plays a triggering or permissive role in tumor recurrence, there is convincing evidence that a new network of capillaries must accompany that tumor growth and recurrence. Tumor angiogenesis is a complex process involving intricate interplay between cells, soluble factors, and extracellular matrix components. The neocapillaries not only provide nutrients for growing tumor cells but also a route of spread and infiltration far beyond the site of the parent tumor (18). If a tumor cannot establish its own blood supply, it ceases to grow and loses power to invade adjacent normal tissue. Interestingly, high-grade gliomas rarely, if ever, metastasize outside the CNS. Rather, they tend to remain local and infiltrate along the vascular networks with or without disturbance of the brain cytoarchitecture. Therefore, angiogenesis and infiltration are interrelated events promoting both survival and recurrence of gliomas. Kinetic studies of glial neoplasms show that a significant fraction of the tumor cells are in a nonproliferating state (19, 20) so that angiogenesis, more than mitosis, characterizes biological aggressiveness and malignancy of primary glial neoplasms of the brain (21). The degree of angiogenesis is an important parameter in assessing the grading of gliomas and, therefore, the degree of malignancy (22).

Treatment of recurrent malignant gliomas is rarely completely successful, because radical surgical resection is nearly always subtotal and chemotherapy/irradiation are mainly palliative rather than curative (23). Many different chemotherapeutic agents have been used to treat recurrent malignant gliomas, but the results have been disappointing. There are two primary reasons for chemotherapeutic failure. First, a significant fraction of the tumor cells are in a nonproliferating state, rendering them resistant to systemic chemotherapy because antimitotic agents, such as carboplatin or procarbazine, and gene therapy or immunotherapy primarily target proliferating cells (24–27). Second, gliomas are often infiltrative. To a great extent, highly mobile infiltrating tumor cells render previously discussed chemotherapeutic agents ineffective. These infiltrating glioma cells usually spread along the white matter tracts without disturbing either the blood-brain barrier (BBB) or brain cytoarchitecture, and then the difference between tumor and normal cells becomes less obvious. Therefore, systemic chemotherapy may not be able to reach these cells scattered among, and camouflaged in, a wide area of normal glial cells. In addition, lack of sufficient BBB breakdown may impede adequate delivery of the chemotherapeutic agent to the remote tumor site. Furthermore, conventional chemotherapeutic agents cause severe myelosuppression, thereby limiting the therapeutic dose (24, 28–30).

As described above, one of the essential features of malignant gliomas is angiogenesis. It therefore appears logical to treat gliomas with antiangiogenic agents, such as thalidomide. Thalidomide was originally developed as a sedative in the 1950s and was withdrawn almost a decade later because of its teratogenic effects on human fetuses (31). Renewed interest in the drug arose in 1964, when a dermatologist from Israel serendipitously discovered that the antiinflammatory properties of thalidomide could be used to treat dermal vasculitis in leprosy (32). Since then, thalidomide has been extensively reinvestigated for other clinical uses and has been shown to have antiinflammatory, immunosuppressive, and antiangiogenic properties (33–36). In 1994, D'Amato et al (5) demonstrated that thalidomide inhibited corneal neovascularization in rabbits. Thalidomide-treated corneal neovascularization was shown to have similar endothelial ultrastructural changes to those seen in the deformed limb bud vasculature of thalidomide-exposed embryos. Recently, the potential role of thalidomide in the treatment of pathologic angiogenesis, such as occurs in diabetic retinopathy, neointimal hyperplasia, and solid tumors, has been investigated (7, 37, 38). In addition, phase I clinical trials of thalidomide for high-grade glial neoplasms have borne encouraging preliminary results (8).

Although not a new drug, thalidomide is a novelty to the vast armamentarium of cancer therapy. The Food and Drug Administration only recently approved it with unprecedented restrictions aimed at avoiding the birth defects caused by thalidomide in the 1950s and 1960s (31, 39). Thalidomide is a proved antiangiogenic agent that has enormous potential for treatment of solid tumors that depend on angiogenesis for growth and survival (5). Aside from its teratogenic effects, the major toxic reaction to orally administered thalidomide is lethargy, which is better tolerated than myelosuppression (40). Recent studies in antiangiogenic cancer therapy using angiostatin, a fragment of plasminogen and an endogenous inhibitor of neovascularization, have shown complete regression of solid tumors in mice (41, 42). Although these laboratory results are not proof of efficacy in humans, the concept of antiangiogenic treatment has revolutionized cancer research and therapeutics, providing another route to thwart the growth of tumors. Endothelial cells cannot become resistant to cancer therapy because, although they are actively growing/proliferating cells, they are not cancer cells. Therefore, drug resistance, one of the most common reasons for chemotherapeutic failure, can potentially be circumvented.

Contrast-enhanced MR imaging plays an essential role in detecting tumor recurrence, in accurately assessing tumor extent, in characterizing tumor progression during therapy, in differentiating tumor from radiation or chemotherapy necrosis, and in distinguishing between tumor-infiltrated parenchyma and vasogenic edema. All these aspects of tumor characterization are important in monitoring response to therapy and, thus, in determining patient management. This role is hampered, however, by the difficulty in distinguishing between tissue necrosis, caused by previous surgical and/or medical therapy, and active tumor (43). Changes seen on T1- and T2-weighted images are highly nonspecific and cannot distinguish among areas of therapy-related changes, edema, and active tumor. Contrast-enhanced MR imaging is an essential tool in the diagnosis and evaluation of primary brain tumors (44, 45). Conventional contrast enhancement in MR imaging, although not completely understood, is related to both disruption and absence of the BBB and proliferation of the microvasculature (46). Alterations in the BBB can occur in aggressive tumors but are also common in areas of necrosis that develop after surgical resection and radiation and/or chemotherapy. Furthermore, aggressive invasion of malignant gliomas does not always destroy the BBB but rather insinuates between white matter tracts, causing only minor alterations in surrounding brain cytoarchitecture (47). Moreover, when high-grade gliomas recur, they tend to invade and replace adjacent tissues rather than expand and increase in size (48). Smith et al (49) described a ''flare phenomenon'' in recurrent high-grade astrocytomas immediately after intralesional immunotherapy, in which there was a transient increase in nodular contrast enhancement, edema, and mass effect. These imaging features resolved without therapy within 3 months, thus con-

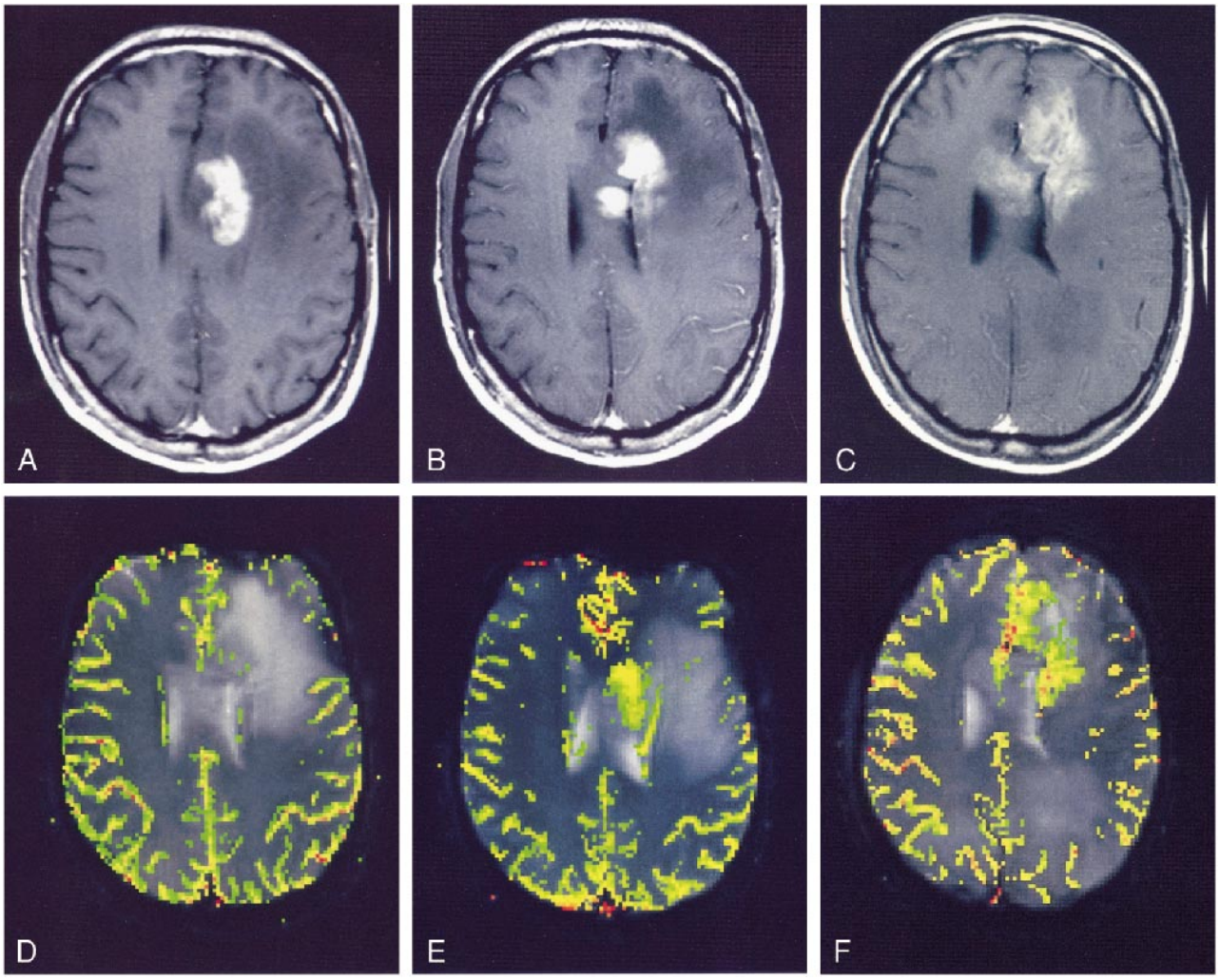

FIG 3. Case 6: 46-year-old-man with left medial frontal anaplastic oligoastrocytoma treated with carboplatin and thalidomide, without concomitant steroid therapy.

A–C, Postcontrast T1-weighted images. At the start of therapy, a solid enhancing mass is seen in the left medial frontal lobe (*A*). At 3-month follow-up, there is a slight increase in contrast enhancement (*B*). At 8-month follow-up, there is a less solid and more linear pattern of enhancement (*C*).

D–F, Corresponding color overlay images. At the start of therapy, there is minimal hyperperfusion, corresponding to the left medial frontal enhancing tumor (*D*). At 3-month follow-up, there is an increase in hyperperfusion (*E*). At 8-month follow-up, there is further progression of hyperperfusion, corresponding well with patient's deteriorating clinical status (*F*).

firming its nonneoplastic nature. On the other hand, these imaging findings could very well represent active tumor growth due to treatment failure. It is thus difficult to follow progression of tumor recurrence and effectiveness of treatment with conventional contrast-enhanced MR imaging alone.

Results of our study confirm the difficulty in assessing tumor progression solely on the basis of conventional postcontrast T1-weighted images, particularly when previous irradiation and/or extensive chemotherapy can complicate image interpretation. As exemplified in our study, almost all recurrent tumors show a progressive increase in contrast enhancement during therapy, which may be due to tumor progression, therapy-related necrosis, or both.

Advanced MR techniques, such as proton MR spectroscopy and apparent diffusion coefficient (ADC) maps, have proved to be helpful in characterizing brain tumors (50–55). Proton MR spectroscopy may provide information concerning metabolic changes associated with tumor growth and degree of malignancy. The single-voxel technique, however, may be inadequate to fully evaluate high-grade glial tumors that are heterogeneous in nature and may, in fact, give erroneous or misleading results. To perform comprehensive examination of high-grade glial tumors, a multivoxel or chemical shift imaging technique is necessary. This technique, however, requires relatively long imaging time and operator-dependent postprocessing. In addition, the resultant spectral patterns may be nonspecific. Measurements of ADC within a tumor may allow characterization of tumor cellularity and, possibly, the degree of malignancy. This technique has mainly been used to differentiate various

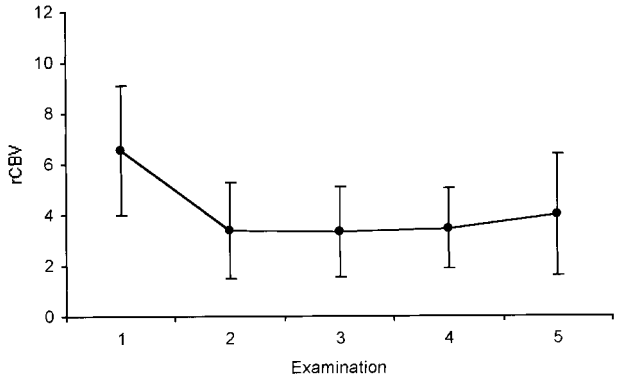

FIG 4. Serial rCBV measurements at each follow-up examination for all patients receiving thalidomide and carboplatin. The interval between each examination varied from 2 to 3 months. The first examination was at the start of the therapy and the fifth examination was at the 12-month follow-up. The decrease in rCBV measurements between the initial and first follow-up examination was statistically significant ($P = .0014$).

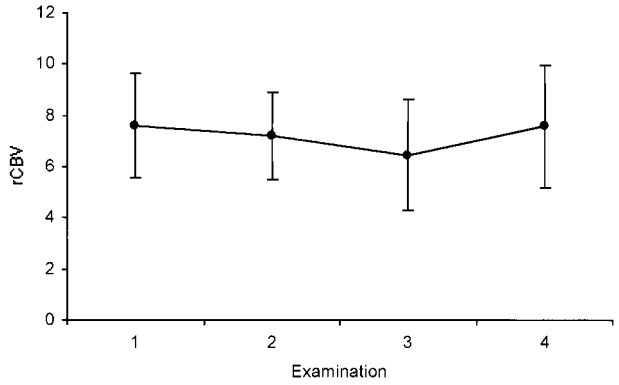

FIG 5. Serial rCBV measurements for patients receiving carboplatin only. There was no statistically significant change in rCBV during the course of therapy.

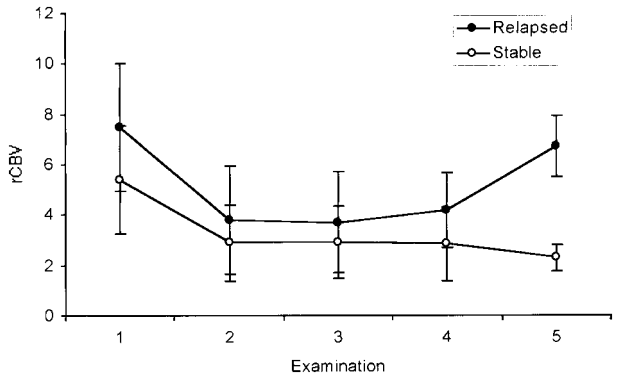

FIG 6. Serial rCBV measurements between the relapsed and the stable groups show a statistically significant difference in rCBV ($P = .0161$) at the 12-month follow-up (ie, the fifth examination), where the relapsed group had higher values than the stable group.

types of intracranial tumors with varying amounts of cellularity but has not been used clinically for assessing posttherapeutic changes. The actual measurement of ADC values is labor-intensive and may not necessarily provide diagnostic information.

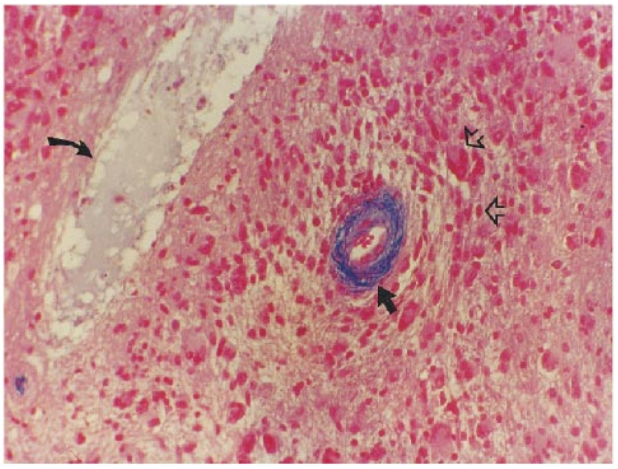

FIG 7. Azocarmine stain from a patient (case 7) with recurrent GBM who was treated with carboplatin and thalidomide shows multilayered reduplication of the basal lamina around a microvessel (*solid straight arrow*). Around this vascular channel, there are several mono- or multinucleated tumor cells (*open arrows*). Adjacent is a tumor microcyst (*curved arrow*).

Recent developments in MR imaging technology allow the semiquantitative assessment of CBV (11, 14, 56), which, in turn, allows noninvasive evaluation of the overall vascularity of a tumor and therefore its aggressiveness and proliferative potential (11). Moreover, noninvasive quantification of vascularity may allow differentiation between a neoplastic process, involving angiogenesis, and therapy-related necrosis, which is an inflammatory process without concomitant neovascularization.

At our institution, contrast-enhanced perfusion MR imaging has been a routine imaging sequence for diagnosis and follow-up of intracranial neoplasms. This technique is fast (60-second acquisition time) and robust, with semiautomated postprocessing that decreases operator-dependent bias. We use multivoxel proton MR spectroscopy as more of a problem-solving tool in conjunction with perfusion-weighted MR imaging and for cases in which susceptibility artifacts hamper interpretation of perfusion-weighted images. The perfusion-weighted MR technique would allow early detection of recurrence and accurate assessment of treatment effectiveness. More important, this technique may, in the future, allow differentiation between active tumor and therapy-related necrosis. Perfusion-weighted MR imaging adds a new dimension to the characterization of tumor progression by providing the vascular status of the tumor. Breakdown of the BBB can cause errors in estimations of rCBV with this method. The baseline correction method we used should help reduce these errors, but it is approximate. Alternative methods for deriving perfusion data, such as measurement of blood flow, may also help, but require measurement of the arterial input function (57). Spin-tagging methods (58–60) avoid the problem by using a freely diffusible tracer, but are currently not widely available, are generally single-slice methods, and are too

noisy for routine clinical use. Despite potential errors, we have previously found that our rCBV measurements correlate well with pathologic findings.

In our study, the perfusion data corresponded much better with the actual clinical status of the patient than did conventional imaging findings. Since therapy-related necrosis is a relatively hypovascular or avascular process, perfusion imaging may better distinguish between necrosis and active tumor. At the 12-month follow-up, those nine patients who were clinically stable without evidence of tumor progression had significantly lower rCBV values than did those with clinical deterioration due to tumor progression. Of those nine patients, seven (78%) are still alive, without further progression of their disease 17 months from the time of recurrence, and their rCBV measurements remain stable. The remaining two patients had marked increases in rCBV along with clinical deterioration at the 15-month follow-up and underwent reoperation.

In the four cases of reoperated tumors, pathologic evaluation showed evidence of both tumor progression and vascular changes compatible with radiation injury. The morphology of tumor capillaries demonstrated both radiation-related fibrinoid necrosis and periadventitial fibroblastic proliferations around the vessel wall, characteristic of radiation-induced vasculopathy. There were bizarre structural alterations of the endothelium, reminiscent of the disorganized vasculature seen in thalidomide-treated rabbit cornea (5), and distinct prominence of hyalinization and extracellular matrix deposition around the vessel wall, which was atypical for radiation-induced vascular injury (Fig 7). In addition, there was multilayered reduplication of the basal lamina of the endothelium, suggestive of aborted angiogenesis in all four cases. The significance of the aforementioned pathologic findings, albeit inconclusive, is that thalidomide may have a role in controlling angiogenesis in human brain tumors. Because of the small number of patients in whom pathologic findings were available, it is premature at this stage to conclude that thalidomide caused these vascular changes. Further work is necessary to differentiate between vascular injury due to radiation and thalidomide.

Not all patients with recurrent malignant gliomas will respond to an antiangiogenic agent such as thalidomide. In such cases, the inability of thalidomide to control tumor growth may be in part due to a lack of sustained antiangiogenic response caused by immune modulation and adaptation of the tumor. Alternatively, in some tumors, florid angiogenesis may be a late phenomenon in tumor growth and recurrence, rendering thalidomide ineffective in the face of widespread tumor infiltration. Nonetheless, perfusion-weighted MR imaging is helpful in the management of patients by accurately depicting the vascular status of the tumor during therapy and, hence, in assessing the effectiveness of treatment. With further research and development in the field of antiangiogenic cancer therapy, perfusion-weighted MR imaging will play an important and active role in determining the efficacy of therapy and in guiding patient management.

Conclusion

Perfusion-weighted MR imaging findings correlated with the patient's clinical status much better than did the findings at conventional postcontrast T1-weighted imaging. Moreover, postcontrast T1-weighted images may be misleading because abnormal enhancement is nonspecific and cannot differentiate between tumor progression and therapy-related changes. Perfusion-weighted MR imaging can reveal changes in tumor vascularity, allowing better evaluation of tumor response and adequacy of therapy than is possible with conventional MR imaging methods. With complementary anatomic localization and physiological information, perfusion-weighted MR imaging is helpful in monitoring tumor response to antiangiogenic drugs such as thalidomide.

References

1. Chang SM, Prados MD. **Chemotherapy for gliomas.** *Curr Opin Oncol* 1995;7:207–213
2. Balmaceda C, Fetell MR, Hesdorffer C. **Thiotepa and etoposide treatment of recurrent malignant gliomas: phase I study.** *Cancer Chemother Pharmacol* 1997;40:72–74
3. Friedman HS, Schold SC Jr, Djang WT, et al. **Criteria for termination of phase II chemotherapy for patients with progressive or recurrent brain tumor.** *Neurology* 1989;39:62–66
4. Burger P. **Malignant astrocytic neoplasms: classification, pathology, anatomy, and response to therapy.** *Semin Oncol* 1986; 13:16–20
5. D'Amato RJ, Loughnan MS, Flynn E, et al. **Thalidomide is an inhibitor of angiogenesis.** *Proc Natl Acad Sci U S A* 1994;91: 4082–4085
6. D'Arcy PF, Griffin JP. **Thalidomide revisited.** *Adverse Drug React Toxicol Rev* 1994;13:65–76
7. Moreira AL, Friedlander DR, Shif B, et al. **Thalidomide and a thalidomide analogue inhibit endothelial cell proliferation in vitro.** *J Neurooncol* 1999;43:109–114
8. Fine HA. **Novel biologic therapies for malignant gliomas: antiangiogenesis, immunotherapy, and gene therapy.** *Neurol Clin* 1995;13:827–846
9. Glass J, Gruber ML, Nirenberg A. **Phase I/II study of carboplatin and thalidomide in recurrent glioblastoma multiforme (abstract).** *Proc Am Soc Clin Oncol* 1999;18:144a
10. Knopp EA, Cha S, Johnson G, et al. **Glial neoplasms: dynamic contrast-enhanced T2*-weighted MR imaging.** *Radiology* 1999; 211:791–798
11. Aronen HJ, Gazit IE, Louis DN, et al. **Cerebral blood volume maps of gliomas: comparison with tumor grade and histologic findings.** *Radiology* 1994;191:41–51
12. Ernst TM, Chang L, Witt MD, et al. **Cerebral toxoplasmosis and lymphoma in AIDS: perfusion MR imaging experience in 13 patients.** *Radiology* 1998;208:663–669
13. Press W, Flannery B, Teukolsky S, et al. ***Numerical Recipes in C: The Art of Scientific Computing.*** Cambridge: Cambridge University Press; 1988
14. Rosen BR, Belliveau JW, Vevea JM, et al. **Perfusion imaging with NMR contrast agents.** *Magn Res Med* 1990;14:249–265
15. Macdonald D, Cascino T, Schold SJ, et al. **Response criteria for phase II studies of supratentorial malignant glioma.** *J Clin Oncol* 1990;8:1277–1280
16. Burger PC, Vogel FS, Green SB, et al. **Glioblastoma multiforme and anaplastic astrocytoma: pathologic criteria and prognostic implications.** *Cancer* 1985;56:1106–1111
17. Brem S. **The role of vascular proliferation in the growth of brain tumors.** *Clin Neurosurg* 1976;23:440–453

18. Scherer HJ. **The forms of growth in gliomas and their practical significance.** *Brain* 1940;63:1–35
19. Hoshino T. **Cell kinetics of glial tumors.** *Rev Neurol* 1992;148: 396–401
20. Nagashima T, Hoshino T. **A review of cell kinetic studies on brain tumors with special reference to anti-bromodeoxyuridine monoclonal antibody method.** *No Shinkei Geka* 1984;12: 1007–1018
21. Maxwell M, Naber SP, Wolfe HJ, et al. **Expression of angiogenic growth factor genes in primary human astrocytomas may contribute to their growth and progression.** *Cancer Res* 1991;51: 1345–1351
22. Kleihues P, Soylemezoglu F, Schauble B, et al. **Histopathology, classification, and grading of gliomas.** *Glia* 1995;15:211–221
23. Obwegeser A, Ortler M, Seiwald M, et al. **Therapy of glioblastoma multiforme: a cumulative experience of 10 years.** *Acta Neurochir* 1995;137:29–33
24. Gruber ML, Glass J, Choudhri H, et al. **Carboplatin chemotherapy before irradiation in newly diagnosed glioblastoma multiforme.** *Am J Clin Oncol* 1998;21:338–340
25. Jeremic B, Grujicic D, Jevremovic S, et al. **Carboplatin and etoposide chemotherapy regimen for recurrent malignant glioma: a phase II study.** *J Clin Oncol* 1992;10:1074–1077
26. Kruse CA, Cepeda L, Owens B, et al. **Treatment of recurrent glioma with intracavitary alloreactive cytotoxic T lymphocytes and interleukin-2.** *Cancer Immunol Immunother* 1997;45:77–87
27. Hayes RL, Koslow M, Hiesiger EM, et al. **Improved long term survival after intracavitary interleukin-2 and lymphokine-activated killer cells for adults with recurrent malignant glioma.** *Cancer* 1995;76:840–852
28. Cloughesy TF, Gobin YP, Black KL, et al. **Intra-arterial carboplatin chemotherapy for brain tumors: a dose escalation study based on cerebral blood flow.** *J Neurooncol* 1997;35:121–131
29. Poisson M, Pereon Y, Chiras J, et al. **Treatment of recurrent malignant supratentorial gliomas with carboplatin (CBDCA).** *J Neurooncol* 1991;10:139–144
30. Twelves CJ, Ash CM, Miles DW, et al. **Activity and toxicity of carboplatin and iproplatin in relapsed high-grade glioma.** *Cancer Chemother Pharmacol* 1991;27:481–483
31. Lenz W. **A short history of thalidomide embryopathy.** *Teratology* 1988;38:203–215
32. Sheskin J. **Further observation with thalidomide in lepra reactions.** *Lepr Rev* 1965;36:183–187
33. Schroder JM, Sellhaus B, Wohrmann T, et al. **Inhibitory effects of thalidomide on cellular proliferation, endoneurial edema and myelin phagocytosis during early wallerian degeneration.** *Acta Neuropathol* 1995;89:415–419
34. Corral LG, Muller GW, Moreira AL, et al. **Selection of novel analogs of thalidomide with enhanced tumor necrosis factor alpha inhibitory activity.** *Mol Med* 1996;2:506–515
35. Klausner JD, Makonkawkeyoon S, Akarasewi P, et al. **The effect of thalidomide on the pathogenesis of human immunodeficiency virus type 1 and M. tuberculosis infection.** *J Acquir Immune Defic Syndr Hum Retrovirol* 1996;11:247–257
36. Mellin G, Katzenstein M. **The saga of thalidomide: neuropathy to embryopathy, with case reports and congenital abnormalities.** *N Engl J Med* 1962;23:1184–1190
37. Minchinton AI, Fryer KH, Wendt KR, et al. **The effect of thalidomide on experimental tumors and metastases.** *Anticancer Drugs* 1996;7:339–343
38. Zwingenberger K, Wnendt S. **Immunomodulation by thalidomide: systematic review of the literature and of unpublished observations.** *J Inflamm* 1996;46:177–211
39. McBride W. **Thalidomide and congenital abnormalities (Letter).** *Lancet* 1961;1358
40. Sheskin J. **The treatment of lepra reaction in lepromatous leprosy: fifteen years' experience with thalidomide.** *Int J Dermatol* 1980;19:318–322
41. O'Reilly MS, Holmgren L, Chen C, et al. **Angiostatin induces and sustains dormancy of human primary tumors in mice.** *Nat Med* 1996;2:689–692
42. Wu Z, O'Reilly MS, Folkman J, et al. **Suppression of tumor growth with recombinant murine angiostatin.** *Biochem Biophys Res Commun* 1997;236:651–654
43. Forsting M, Albert FK, Kunze S, et al. **Extirpation of glioblastomas: MR and CT follow-up of residual tumor and regrowth patterns.** *AJNR Am J Neuroradiol* 1993;14:77–87
44. Felix R, Schorner W, Laniado M, et al. **Brain tumors: MR imaging with gadolinium-DTPA.** *Radiology* 1985;156:681–688
45. Bird CR, Drayer BP, Medina M, et al. **Gd-DTPA-enhanced MR imaging in pediatric patients after brain tumor resection.** *Radiology* 1988;169:123–126
46. Sage MR. **Blood-brain barrier: phenomenon of increasing importance to the imaging clinician.** *AJR Am J Roentgenol* 1982; 138:887–898
47. Alvord EJ, Shaw C-M, Richards T. **The relative rates of cellular proliferation and infiltration and the histologic definition of gliomas.** *Can J Neurol Sci* 1993;20:83
48. Tracqui P, Cruywagen GC, Woodward DE, et al. **A mathematical model of glioma growth: the effect of chemotherapy on spatiotemporal growth.** *Cell Prolif* 1995;28:17–31
49. Smith M, Thompson J, Castillo M, et al. **MR of recurrent high-grade astrocytomas after intralesional immunotherapy.** *AJNR Am J Neuroradiol* 1996;17:1065–1071
50. Castillo M, Kwock L, Mukherji SK. **Clinical applications of proton MR spectroscopy.** *AJNR Am J Neuroradiol* 1996;17:1–15
51. Castillo M, Kwock L, Scatliff J, et al. **Proton MR spectroscopy in neoplastic and non-neoplastic brain disorders.** *Magn Reson Imaging Clin N Am* 1998;6:1–20
52. Taylor JS, Langston JW, Reddick WE, et al. **Clinical value of proton magnetic resonance spectroscopy for differentiating recurrent or residual brain tumor from delayed cerebral necrosis.** *Int J Radiat Oncol Biol Phys* 1996;36:1251–1261
53. Wald LL, Nelson SJ, Day MR, et al. **Serial proton magnetic resonance spectroscopy imaging of glioblastoma multiforme after brachytherapy.** *J Neurosurg* 1997;87:525–534
54. Sugahara T, Korogi Y, Kochi M, et al. **Usefulness of diffusion-weighted MRI with echo-planar technique in the evaluation of cellularity in gliomas.** *J Magn Reson Imaging* 1999;9:53–60
55. Krabbe K, Gideon P, Wagn P, et al. **MR diffusion imaging of human intracranial tumours.** *Neuroradiology* 1997;39:483–489
56. Edelman RR, Mattle HP, Atkinson DJ, et al. **Cerebral blood flow: assessment with dynamic contrast-enhanced T2*-weighted MR imaging at 1.5 T.** *Radiology* 1990;176:211–220
57. Ostergaard L, Sorensen AG, Kwong KK, et al. **High resolution measurement of cerebral blood flow using intravascular tracer bolus passages, II: experimental comparison and preliminary results.** *Magn Reson Med* 1996;36:726–736
58. Detre JA, Leigh JS, Williams DS, et al. **Perfusion imaging.** *Magn Reson Med* 1992;23:37–45
59. Edelman RR, Siewert B, Darby DG, et al. **Qualitative mapping of cerebral blood flow and functional localization with echo-planar MR imaging and signal targeting with alternating radio frequency.** *Radiology* 1994;192:513–520
60. Kim SG. **Quantification of relative cerebral blood flow change by flow-sensitive alternating inversion recovery (FAIR) technique: application to functional mapping.** *Magn Reson Med* 1995;34:293–301